SPE-179678-MS

Design of a Robust ASP Formulation for Clay Rich and Moderate Permeability Sandstone Reservoir: From Laboratory to Single Well Chemical Tracer Test in the Field

Neeraj Rohilla, TIORCO, a Nalco Champion Company; Ravi Ravikiran, Stepan Company; Charlie T. Carlisle, Chemical Tracers Inc.; Nick Jones, University of Wyoming; Marron B. Davis, Sunshine Valley Petroleum Corporation; Kenneth B. H. Finch, TIORCO, a Nalco Champion Company

This paper was prepared for presentation at the SPE Improved Oil Recovery Conference held in Tulsa, Oklahoma, USA, 11–13 April 2016.

Abstract

Sandstone reservoirs containing significant amount of clays (30-40 wt%) with moderate permeability (20-50 mD) provide a unique challenge to surfactant based enhanced oil recovery (EOR) processes. A critical risk factor for these types of reservoirs is adsorption of surfactants due to greater surface area attributed to clays. Clays also have high cation exchange capacity (CEC) and can release significant amounts of di-valents that lead to increased retention of the surfactant. These factors could adversely affect the economics of a flood.

We present a case study where a robust formulation was designed and tested in lab/field for a reservoir located in Wyoming, USA and contains up to 35-40 wt% clays (predominately Kaolinite and Illite). The residual oil saturation is high (Sor=0.4) while the permeability of the formation is between 20-50 mD. The reservoir has been waterflooded historically with low salinity water which has led to formation permeability damage. Due to high levels of clays, adsorption of the surfactant on the rock surface was determined to be between 3-4 mg/g rock by static adsorption tests.

This publication demonstrates how the following challenges have been successfully addressed in the lab as well as in the field in the form of single well chemical tracer test (SWCTT).

1. Designed a robust alkaline-surfactant-polymer (ASP) formulation that showed ultra-low interfacial tension (IFT) values and aqueous solubility remains soluble in the aqueous solution over a broad range of salinity.
2. Mitigated surfactant adsorption issues to make the cEOR solution economic. A sacrificial agent was identified that acted synergistically with alkali and also did not alter the optimum salinity of the formulation.
3. Performed restored state core analysis using the available damaged core material. The main challenge being restoration of the coreplugs to current reservoir conditions for coreflood experiment without causing additional formation damage due to injection of low salinity formation brine.

4. Designed a flood that utilized a pre-flush to provide a favorable salinity gradient and to inject sacrificial agent ahead of the surfactant front.
5. Performed polymer screening to select right molecular weight of polymer so that the right balance of mobility control and injectivity in the reservoir can be obtained.

Introduction

In a chemical flood, surfactant cost is a key cost element to overall project economics. The majority of the injected surfactant into a reservoir is lost due to adsorption on the reservoir rock surface. Sandstone reservoirs have a net negative charge at neutral pH. Therefore, anionic surfactants are preferred over nonionic or cationic surfactants because of lower adsorption on the sandstone reservoir rock. If reservoir brine does not contain significant amounts of Ca/Mg, then alkali can be used to further reduce the adsorption (Liu et al. 2008; Hirasaki et al. 2011).

The presence of clays in sandstone usually leads to increased adsorption/retention of the surfactant by two different mechanisms. High surface area clays provide excess surface for surfactant molecules/micelles to adsorb. Moreover, clays also have high cation exchange capacity (CEC). When the equilibrium between formation brine and reservoir rock is disturbed due to changes in salinity, some clay release significant amounts of di-valents (Griffith, 1978). This can lead to increased retention/loss of the surfactant (Wilson and Pittman, 1977; Langmuir, 1997; Velde and Meunier, 2008).

Reservoir rock/fluid characterization:

The field is located in the state of Wyoming, USA. The field was discovered in 1919 and has since produced approximately 32.1 MMbbls oil. There are up to seven separate oil bearing intervals in the formation area. The clays found include kaolinite, chlorite, mixed-layer illite/smectite, mixed-layer illite/mica, and smectite. The kaolinite in the formation is authigenic, a result of the diagenetic alteration of K-feldspar (Stone, 1972). In some instances, reservoir rock consists of 35-50 wt% clay as shown in Figures 1–4 (Jones et al. 2013). The dominant lithologies of the formation are bioturbated, very fine to fine-grained white to gray wavy (flaser) bedded sandstones intercalated with dark gray to black mudstones with abundant coalified plant fragments. Minor lithologies include fine grained tan, to yellow crossbedded sandstone, tan and grey to black shale and carbonaceous shale, and white to dark grey clay (bentonites) (Jones et al. 2013).

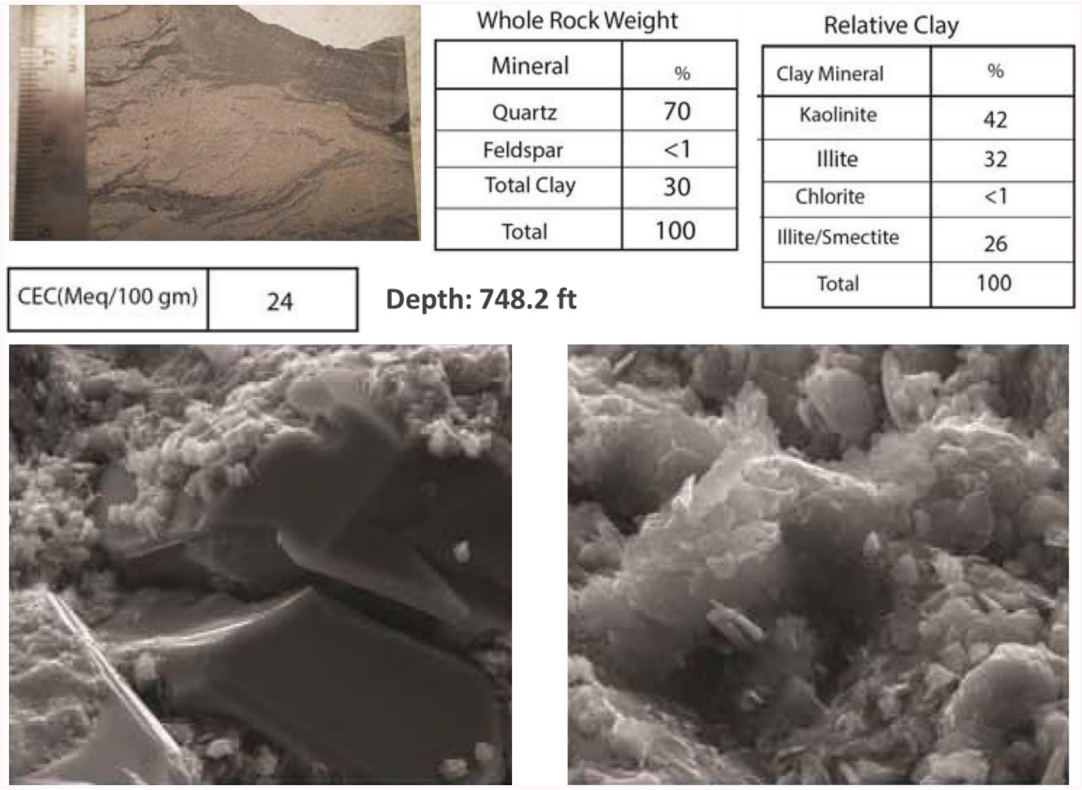

Figure 1—XRD, SEM and CEC analysis for a sample of wavy, laminated, fine-grained sandstone. Authigenic Kaolinite can be observed in some pores of tight laminae (Jones et al. 2013).

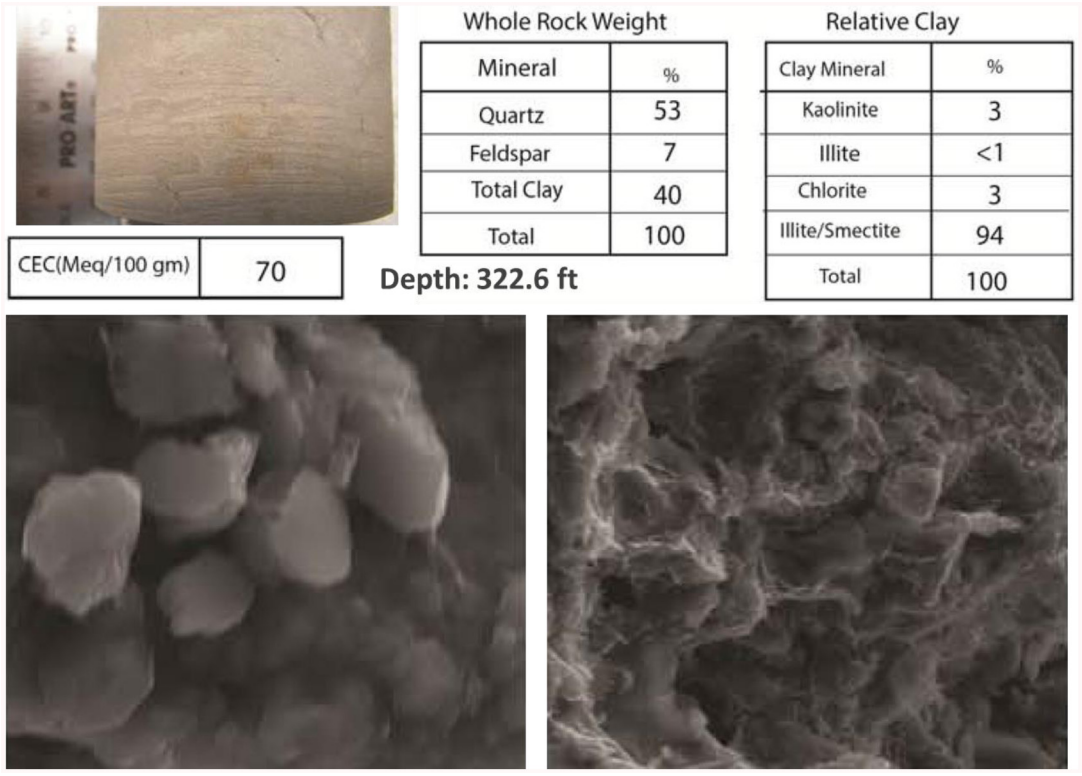

Figure 2—XRD, SEM and CEC analysis for a sample of not well stratified siltstone with abundant clay matrix. Illite/Smectite accounts for majority of the clays (Jones et al. 2013).

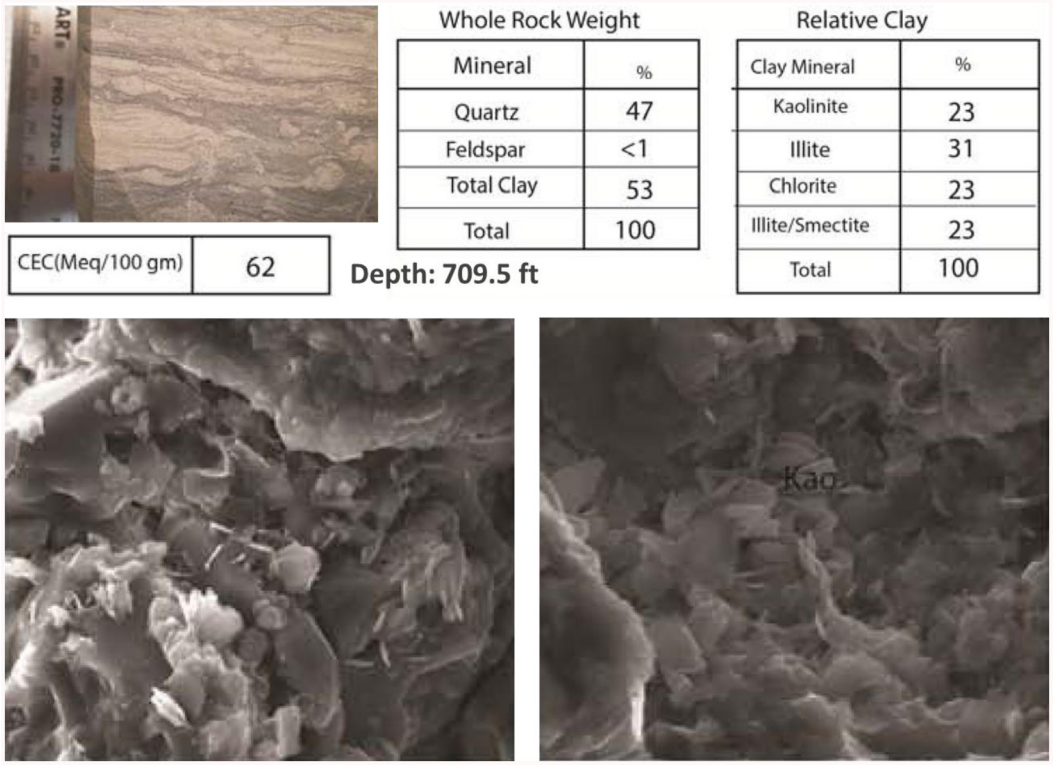

Figure 3—XRD, SEM and CEC analysis for a sample of clay rich shaly sandstone. Authigenic Kaolinite and Illite is observed in SEM images (Jones et al. 2013).

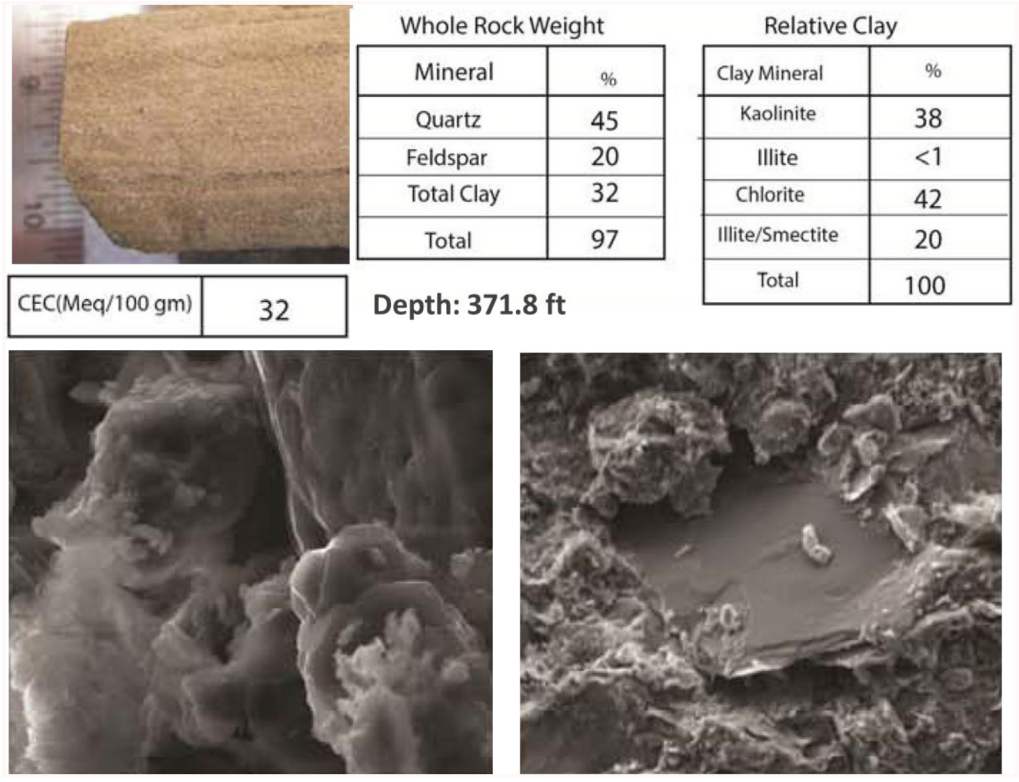

Figure 4—XRD, SEM and CEC analysis for a sample of laminated very fine-grained sandstone with clay-rich laminae. Chlorite/Kaolinite accounts for majority of the clays (Jones et al. 2013).

The temperature of the reservoir is 28 °C and the connate brine is very fresh (1000-3000 ppm TDS) containing small amounts of di-valents. Hence, surfactant formulations with and without alkali (sodium carbonate) were options for this reservoir.

Crude oil in the reservoir is of low viscosity (5-7 cP), 38-40 °API gravity and exhibited very low (0-0.02) total acid number (TAN). Oil analysis of two different samples is shown in Table 1.

Table 1—Characterization of reservoir crude oil from two different wells

	SARA Composition (wt%)						
Sample	SAT	ARO	RESIN	ASPH.	°API	Total acid number (TAN)	Viscosity (cP)
Oil # 1	62.49	31.60	5.66	0.24	39.4	0	4.7
Oil # 2	65.11	30.21	4.45	0.23	39.8	0	4.5

The water composition of available injection water as well as that of the produced water is listed in the Table 2.

Table 2—Water analysis of the field produced water and available injection water

Chararteristic Value	Injection Water	Produced Water
pH (s.u.)	8.13	7.85
Resistivity (Ohm.m)	2127.7	257.7
Calcium Hardness (mg/L as $CaCO_3$)	134	38.0
Total Hardness (mg/L as $CaCO_3$)	239	50.3
CATIONS, mg/L		
Calcium (Ca^{2+})	53.5	15.2
Magnesium (Mg^{2+})	25.7	3.00
Potassium (K^{+})	1.79	2.54
Silicon (Si^{4+})	8.45	4.04
Sodium (Na^{+})	3.70	790
Strontium (Sr^{2+})	0.455	0.419
ANIONS, mg/L		
Chloride (Cl^{-})	0.762	796
Fluoride (F^{-})	0.332	0.705
Nitrate (NO_3^{-})	0.266	0.259
Phosphate (PO_4^{3-})	<3.0	<3.0
Sulfate (SO_4^{2-})	33.2	0.557
Total Alkalinity	291	976
TDS, mg/L (calculated from IC & ICP)	419	2589

Methodology

Materials:

Various agents used in these experiments consist of commercially available surfactants, polymers, alkali and other chemicals.

Experiments:

In order to design a robust surfactant formulation that recovers significant amounts of residual oil post waterflood, the capillary number needs to be increased by at least three orders of magnitude (Taber, 1969; Melrose and Brandner, 1974; Stegemeier, 1977). Lowering the interfacial tension (IFT) between aqueous and oil phase to ultra-low value (10^{-3} dynes/cm or lower) is critical in mobilizing trapped residual oil in the reservoir. Many experiments are needed to find a suitable surfactant formulation for a given reservoir.

Firstly, surfactant phase behavior tests involving either salinity scans or surfactant scans were conducted as high throughput screening tool to select one or many blends of surfactant which can achieve ultra-low IFT values. Then, a robustness study was performed to determine the range of salinity and the surfactant concentrations over which the formulation maintains ultra low IFT values. The criterion for selection was that the formulation be robust enough that any +/- change of 5% in any component does not alter the interfacial interactions significantly.

Secondly, static and dynamic adsorption tests were performed to measure the surfactant adsorption capacity of the rock to ensure enough surfactant is used in coreflood experiments to offset the loss of surfactant to the rock surface. Finally, a series of coreflood experiments were performed to characterize the effectiveness of developed surfactant formulation in displacing residual oil under reservoir conditions. Once confidence in the formulation as established, a single well chemical tracer test (SWCTT) was performed in the field. The following sections describe in details the results of these tests.

Results and Discussion

Surfactant phase behavior tests:

Salinity scans are the most common batch experiments to find the optimum surfactant formulation exhibiting type III microemulsion behavior at the desired salinity. In a salinity scan experiment, typically surfactant/co-solvent concentrations and the water oil ratio (WOR) are kept constant while the salinity is increased systematically for a set of phase tubes (Figures 5 and 6). Increases in salinity causes the classical Winsor surfactant phase behavior transitions from Type I (oil in water microemulsion) to Type III (bi-continuous middle phase microemulsion) to Type II (water in oil) microemulsions (Reed and Healy, 1974; Liu et al. 2008; Bourrel and Schechter, 2010). The surfactant formulation for this project consists of a mixture of two surfactants and a co-solvent. One of the surfactant is an alcohol propoxy sulfate (APS) while the other is an internal olefin sulfonate (IOS). Isobutanol (IBA) is the co-solvent component of the formulation. The formulation consists of 1 wt% total surfactant and 1 wt% co-solvent. Typical salinity scans for the reservoir oil with and without alkali are shown in Figures 5 and 6. For both cases, a middle phase consisting of type III microemulsion is observed. The solubilization ratio at optimal salinity is about 25-30. Such high solubilization ratios suggest ultra low IFT based on Chun-Huh correlation (Huh, 1979).

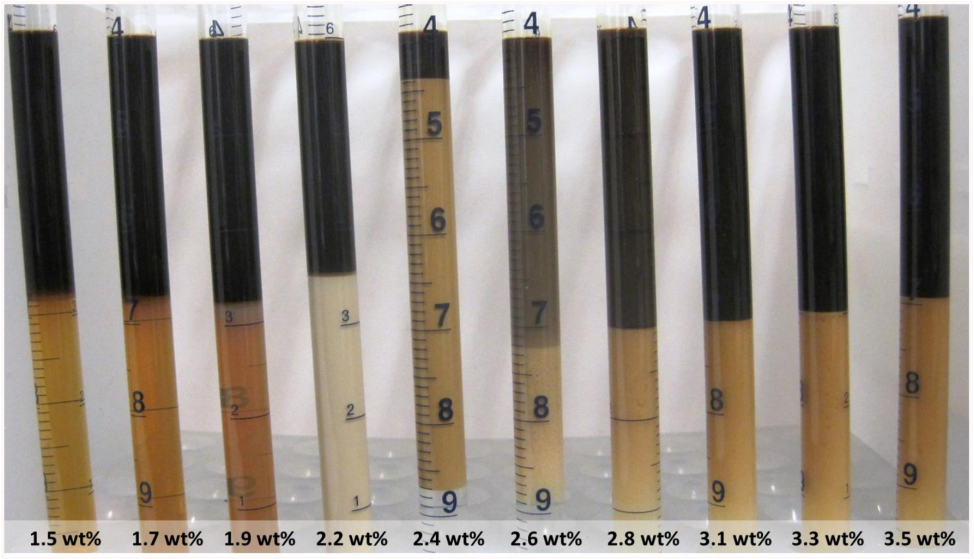

Figure 5—Sodium chloride salinity scan (1.5 wt% to 3.5 wt%) phase behavior test using the 1 wt% surfactant and 1 wt% co-solvent in the aqueous phase.

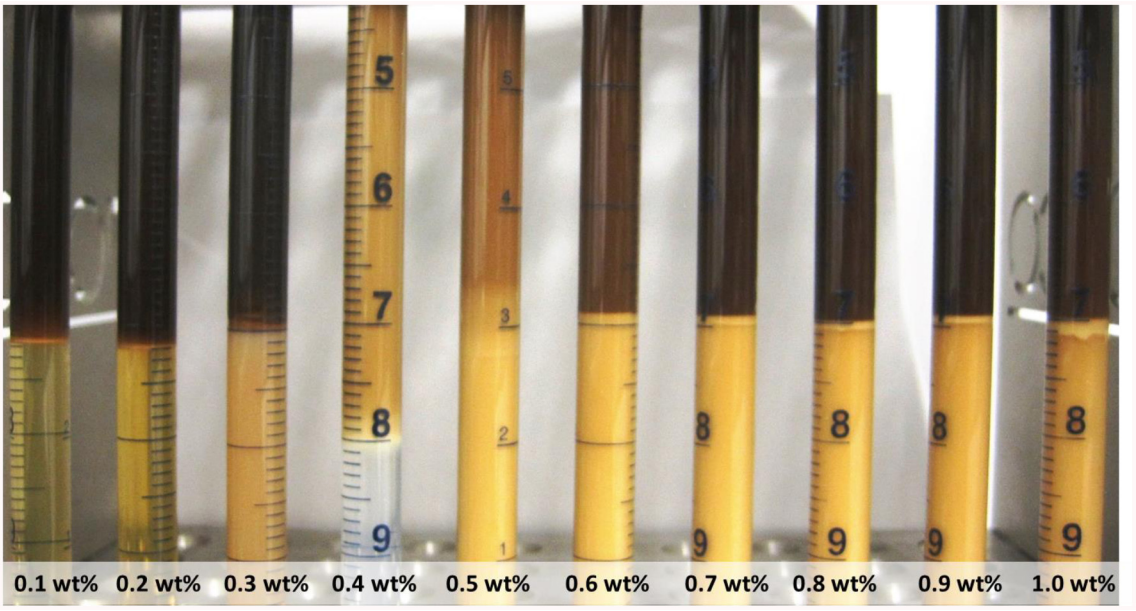

Figure 6—Sodium chloride salinity scan (0.1-1.0 wt%) phase behavior test using the 1.75 wt% sodium carbonate, 1 wt% surfactant and 1 wt% co-solvent in the aqueous phase.

Though, the crude oil is not reactive with alkali as exhibited by low total acid number of the crude oil, alkali (sodium carbonate) is used to reduce the adsorption of surfactant on the rock surface under high pH conditions (Liu et al. 2008). Other phase behavior tests were conducted to compute the activity diagram which show optimal salinity as a function of the surfactant concentration and the water oil ratio (WOR). The best formulation has the optimal salinity of 1.75 wt% Na_2CO_3 + 0.5 wt% NaCl at WOR of 1. The optimal salinity is 1.75 wt% Na_2CO_3 + 0.9 wt% NaCl at WOR of 3. Typically, the residual oil saturation (Sor) in mature sandstone reservoirs is about 1/3. Hence, for this study salinity of the injected ASP slug during corefloods was same as the optimal salinity at WOR of 3.

Table 3 shows the IFT measured using a spinning drop tensiometer. The current formulation yields ultra-low IFT (10^{-3} dynes/cm or lower) over a 5,000 ppm range of salinity. The viscosity of type III microemulsion can have a significant effect on the transport of generated oil bank in porous media during a coreflood (Gogarty et al. 1970). The viscosity of the type III microemulsion phase was measured using a falling sphere viscometer (Lopez-Salinas et al. 2009). Figure 7 shows the viscosity of type III microemulsion phases observed for various formulations during the phase behavior screening tests. For the selected formulation, the viscosity of the type III microemulsion phases was in the range of 6-11 cP.

Table 3—IFT values measured using spinning drop tensiometer for the ASP formulation at 1.0 wt% and 0.5 wt% total surfactant concentration.

Na_2CO_3 (wt%)	NaCl (wt%)	IFT (dynes/cm) for 1.0 wt% Total Surf.	IFT (dynes/cm) for 0.5 wt% Total Surf.
1.75	0.5	0.0013	0.0003
1.75	0.6	0.0022	0.0002
1.75	0.7	0.0015	0.0012
1.75	0.8	0.0004	0.0012

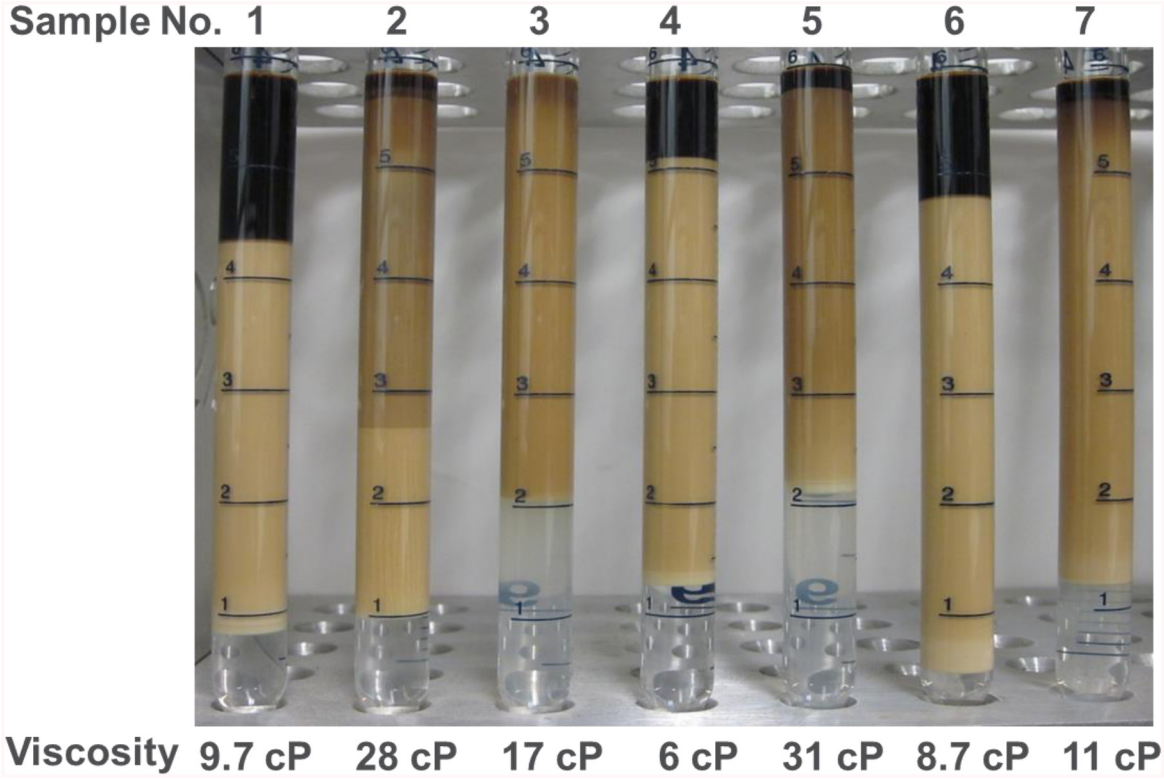

Figure 7—Microemulsions and the associated viscosities measured using falling sphere viscometer.

Surfactant adsorption tests:

Surfactant is the most expensive component of the ASP formulation. An ASP process is designed and optimized with the consideration that a significant portion of the injected surfactant is lost onto the reservoir rock surface. This is deliberately done such that the produced oil bank is not emulsified at the producer well thereby requiring little or no emulsion breaking treatment. Hence, an accurate characterization9678f5;0;3;act/act;ZPICKFOOT;F5?ization of the adsorption capacity of the reservoir rock is necessary to design the appropriate ASP slug size and the concentration of the surfactant in the ASP slug (Sheng, 2010a; Sheng, 2013).

Adsorption test is a technique used to measure the loss of surfactant onto the crushed reservoir rock. When the test is carried out by contacting surfactant solution with crushed reservoir rock under static conditions (no flow), the test is called a ″Static adsorption test″. A similar test conducted under flow conditions through a core is called a ″Dynamic adsorption test″. To estimate the surfactant adsorption, either ″Static″ or ″Dynamic″ adsorption tests are conducted.

In the Static adsorption test, surfactant adsorption can be estimated with batch adsorption experiments. In these experiments, a surfactant solution of known concentration is contacted with a known mass of crushed core materials. Crushed core material between 35-100 mesh sizes (150-500 micron particle size) is used for the current study. The concentration of the equilibrated surfactant solution is measured and the adsorption is computed by a material balance of surfactant using the following equation.

$$Ad\ \left(\frac{mg}{g\ rock}\right) = \frac{\left(W_{Surf.Solution} * 10 * \left(C_i - C_f\right)\right)}{W_{Rock}} \quad \text{Equation 1}$$

Where:

C_i= Initial solution concentration (wt%)

C_f= Final solution concentration (wt%)

$W_{Surf.\ solution}$ = Weight of the surfactant solution in contact with the rock (g)
W_{Rock} = Weight of the crushed rock in contact with surfactant solution (g)

An ionic surfactant adsorption isotherm consists of four different regions as shown in Figure 8 (Koopal et al. 1995). At low surfactant concentrations (Regime I), adsorption density of the surfactant is governed by the electrostatic interactions between charged surfactant molecules and the oppositely charged solid surface. As surfactant concentration is increased, individual surfactant molecules begin to self assemble in the form of aggregates (hemi-micelles, admicelles etc.) resulting in increased adsorption density (Regime II and III). When the surfactant concentration reaches cricitcal micelle concentration (CMC), further increase in surfactant concentration does not change the adsorption density (Koopal et al. 1995). In Chemical EOR, injected surfactant concentrations are well beyond the CMC. Therefore, the operating conditions fall under the plateau region (Regime IV) of the isotherm and surfactant adsorption density reaches a constant value. Because of this, the static adsorption tests are performed at a lower surfactant concentrations (2,000-2,500 ppm, but still greater than the CMC) so that a good resolution between initial and final surfactant concentrations can be obtained.

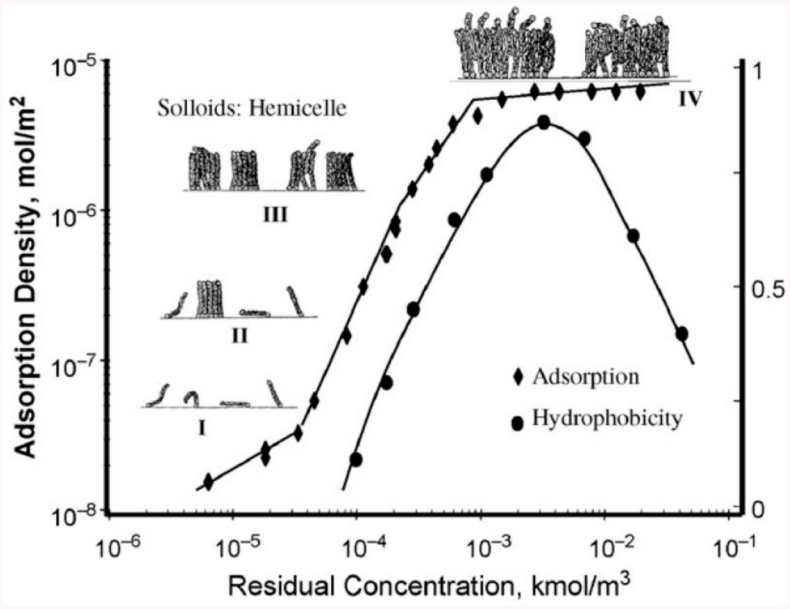

Figure 8—Various regimes of the typical surfactant adsorption isotherm for sodium dodecyl sulfate (SDS) on alumina at pH 6.5 (Koopal et al. 1995; Zheng and Somasundaran, 2006).

It is also assumed that the mechanism of the surfactant transport towards the solid particle surface is not the limiting step. Therefore, the value of the static adsorption (mg surf/g rock) should stay constant when varying the amount of solids and surfactant solution by the same factor. The typical relative error of surfactant concentration measurements in the laboratory is about 5 %. Therefore, the Static adsorption test should be designed in such a way that the change in the initial surfactant concentration due to adsorption is at least 25-30% of the initial concentration.

Surfactant adsorption was calculated for two different samples of the reservoir rock (sample 1 and 2). Table 4 lists the XRD analysis, CEC and the BET surface areas for samples 1 and 2. Sample 1 contains on average of 19 wt% of clays while sample 2 contains 43 wt% of clays. Kaolinite is considered to be mainly responsible for the loss of permeability in reservoirs because it occurs in the morphology of hexagonal shaped booklets blocking the pore throats (Wilson and Pittman, 1977, Velde and Meunier, 2008). Illite and Chlorite usually have higher CEC values than that of Kaolinite and cause higher surfactant adsorption than that caused by Kaolinite.

Table 4—Quantitative XRD analysis, CEC and BET surface areas of two rock samples from different wells of the reservoir.

	Whole Rock Weight (wt%)			Relative Clay Percentages (%)					
Sample #	Quartz	Feldspar	Clay	Kaolinite	Illite	Chlorite	Illite/Smectite	CEC (meq/100 g)	Surface area (m^2/g)
1	72	9	19	47	11	30	12	14	1
2	47	10	43	68	7	<1	25	9	5-6

Tables 5 and 6 list the results of these static adsorption tests performed for the surfactant formulation with rock samples 1 and 2. In the absence of alkali, the surfactant adsorption is quite high (2.3 mg/g for sample #1 and 4.7 mg/g for sample # 2). Alkali only marginally reduces the adsorption and is not an effective adsorption mitigator for the current reservoir rock. The reservoir rock contains significant amounts (Figure 1–4, Table 4) of reactive clays which result in a significant change in pH of the surfactant solutions when contacting the rock. For an ASP process to be economical the surfactant adsorption should be small (less than 0.5 mg/g rock). Adsorption results shown in Tables 5 and 6 suggest the need for a suitable sacrificial agent that can reduce the adsorption significantly in the presence of alkali.

Table 5—Surfactant adsorption for the selected formulation on a representative rock sample # 1 from the reservoir for different surfactant concentration solutions and two different brine compositions.

Rock Sample No.	Brine composition	Co (initial) (ppm)	C* (final) (ppm)	Surfactant Adsorption (mg/g rock)	pH (Initial)	pH (final)
Crushed rock sample 1 (35-100 mesh size)	2.25 wt% NaCl	2,500	1,335	2.3	9.8	7.0
	1.75 wt% Na_2CO_3 + 0.5 wt% NaCl	2,500	1,511	1.9	11.7	11.2
	2.25 wt% NaCl	1,500	267	2.5	9.7	7.1
	1.75 wt% Na_2CO_3 + 0.5 wt% NaCl	1,500	591	1.8	11.6	11.3
	2.25 wt% NaCl	1,000	118	1.8	7.3	7.0
	1.75 wt% Na_2CO_3 + 0.5 wt% NaCl	1,000	172	1.6	11.6	11.3

Table 6—Surfactant adsorption for the selected formulation on a representative rock sample # 2 from the reservoir for a surfactant initial concentration of 2,500 ppm and two different brine compositions.

Rock Sample No.	Brine composition	Co (initial) (ppm)	C* (final) (ppm)	Surfactant Adsorption (mg/g rock)	pH (initial)	pH (final)
Crushed rock sample 2 (35-100 mesh size)	2.25 wt% NaCl	2,500	133	4.7	9.8	5.0
	1.75 wt% Na_2CO_3 + 0.5 wt% NaCl	2,500	269	4.5	11.7	10.9

A sacrificial agent is a chemical that is mixed with surfactant blend and/or is injected ahead of the surfactant front to satisfy the adsorption capacity of the reservoir rock. A sacrificial agent should reduce the surfactant adsorption significantly to offset the added cost of the sacrificial agent. A sacrificial agent should be relatively inert and should not influence crude oil/surfactant/brine interactions by causing a change in optimal salinity or interfacial tension. Researchers in the past have used various chemicals as sacrificial agents such as sodium polyacrylate, glyceric acid, glycolic acid, sodium metaborate, lignin sulfonates, polyethylene glycol (PEG), polypropylene glycol (PPG) etc. to reduce the surfactant adsorption. There are numerous references in the literature that discuss the mechanisms of surfactant adsorption on the solid surface and evaluate various sacrificial agents using static/dynamic adsorption tests (So-

masundaran and Hanna, 1979; Falcone et al. 1982; Osterloh and Jante, 1992; Austad, 1993; Bai and Grigg, 2005; Zheng and Somasundaran, 2006; Shamsijazeyi, 2013).

To screen sacrificial agents to be used for a reservoir containing significant amount of clays, Kaolin powder was used as a model substrate for adsorption studies. Three different sacrificial agents were identified based on preliminary testing. The concentration of the sacrificial agent was the same as the total surfactant concentration. Table 7 shows the results of static adsorption tests performed for surfactant formulation with 100% Kaolin powder. In the absence of any sacrificial agent, the surfactant adsorption was calculated to be 11.9 mg/g rock. Agent C was found to be most effective. Using Agent C as sacrificial agent, the adsorption is reduced by a factor of two on Kaolin powder.

Table 7—Adsorption values of surfactant for 100% Kaolin powder with and without sacrificial agents. The concentration of the sacrificial agent was same as the total surfactant concentration.

S. No.	Sand Type	Brine Composition	Sacrificial Agent	Surfactant Adsorption (mg/g rock)
1	100% Kaolin	1.75 wt% Na_2CO_3 + 0.5 wt% NaCl	None	11.9
2			Agent A	10.9
3			Agent B	8.2
4			Agent C	5.6

Next, we performed series of static adsorption tests to evaluate Agent C as the sacrificial agent with crushed Berea rock. The results are shown in Table 8. Use of alkali reduces the surfactant adsorption from 0.56 mg/g rock to 0.25 mg/g rock. Using sacrificial agent alone in the absence of alkali reduces the surfactant adsorption from 0.56 mg/g rock to 0.14 mg/g rock. However, using the sacrificial agent in the presence of alkali further reduces the adsorption to 0.1 mg/g rock suggesting the synergy between alkali and the sacrificial agent.

Table 8—Adsorption values of surfactant for crushed Berea rock (35-100 mesh size) with and without alkali and sacrificial agents. The concentration of the sacrificial agent was same as the total initial surfactant concentration.

S. No.	Sand Type	Brine Composition	Sacrificial Agent	Surfactant Adsorption (mg/g rock)
1	Crushed Berea Sandstone (35-100 mesh size)	2.25 wt% NaCl	None	0.56
2		1.75 wt% Na_2CO_3 + 0.5 wt% NaCl	None	0.25
3		2.25 wt% NaCl + Agent C	Agent C	0.14
4		1.75 wt% Na_2CO_3 + 0.5 wt% NaCl + Agent C	Agent C	0.1

Finally, we performed a series of static adsorption tests to evaluate all three sacrificial agents with crushed reservoir rock (35-100 mesh size) with and without alkali. The results are shown in Table 9. Use of alkali reduces surfactant adsorption from 2.2 mg/g rock to 1.75 mg/g rock. In the absence of alkali, use of Agents A, B alone reduces the adsorption from 2.2 mg/g rock to 1.82 mg/g rock and 1.31 mg/g rock, respectively. Using Agent C alone reduces the adsorption from 2.2 mg/g rock to 1.08 mg/g rock. However, using Agent C along with alkali reduces the adsorption from 2.2 mg/g rock to 0.41 mg/g rock. This suggests that Agent C and alkali should be used together to minimize the surfactant adsorption.

Table 9—Adsorption values of surfactant for crushed Berea rock (35-100 mesh size) with and without alkali and sacrificial agents. The concentration of the sacrificial agent was same as the total initial surfactant concentration.

S. No.	Sand Type	Brine composition	Surfactant Adsorption (mg/g rock)
1	Crushed Reservoir Rock (35-100 mesh size)	2.25 wt% NaCl	2.2
2		1.75 wt% Na_2CO_3 + 0.5 wt% NaCl	1.75
3		2.25 wt% NaCl + Agent A	1.82
4		2.25 wt% NaCl + Agent B	1.31
5		2.25 wt% NaCl + Agent C	1.08
6		1.75 wt% Na_2CO_3 + 0.5 wt% NaCl + Agent C	0.41

Coreflood experiments and design of the ASP process for the field:

A successful design of the ASP process has three main objectives (Sheng, 2010b, Hirasaki et al. 2011):

1. Surfactant slug to pass through the reservoir at near optimal conditions to ensure ultra low IFT between aqueous and oil phase.
2. Maintain low enough IFT towards the end of the slug such that the mobilized oil doesn't get retrapped when the surfactant experiences dispersion, change in optimal salinity and adsorption to the rock (Hirasaki, 1982; Hirasaki et al. 1983).
3. Ensure good mobility control such that the injected fluids don't finger through the oil bank.

As shown in the Figure 9, the typical pore body size obtained from the mercury porosimetry is between 10-15 micrometers. The typical pore size for a 300 mD Berea core is about 24 microns. It is assumed that the typical pore length scale varies with square root of the permeability (Hirasaki and Pope, 1974; Dullien, 1975). Hence, to match the typical pore size of the outcrop core with that of the reservoir core, a low permeability Berea core (65 mD) was used in the first coreflood. Though, the high permeability (> 300 mD) Berea core is considered homogeneous and free of clay minerals, low permeability Berea core can contains up to 10 wt% Kaolinite/Illite. Hence, low permeability Berea core is a good analog of the reservoir core to evaluate the ASP formulation in a coreflood.

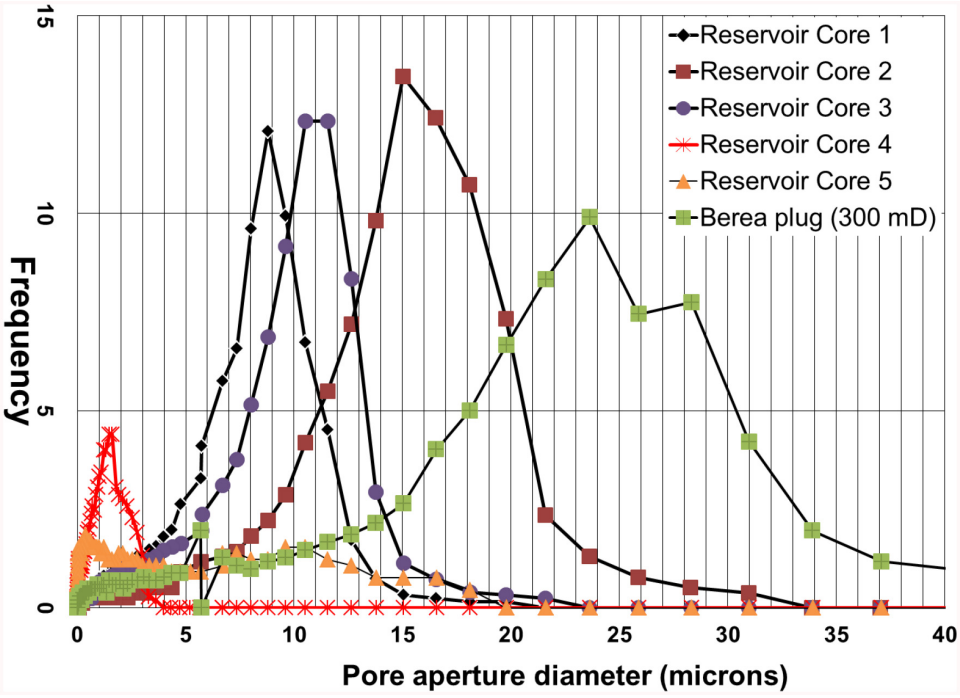

Figure 9—Pore size distribution of several reservoir coreplugs obtained from mercury porosimetry measurements. The pore size distribution of a Berea core of 300 mD permeability is also shown.

Outcrop Berea coreflood: The coreflood procedure follows:

1. Saturate the Berea core with produced field water using vacuum saturation and calculate porosity and the pore volume of the core.
2. Maintain the coreflooding apparatus at reservoir temperature and inject several pore volumes of produced field water, establish the pressure drop baseline and measure the permeability of the whole core as well as that of the individual sections by varying the flowrates.
3. Inject several pore volumes of the reservoir crude oil into the core until the water cut is below 0.5%.
4. Age the core at reservoir temperature for about two weeks.
5. Flush the aged crude oil with 2 PV of fresh reservoir oil.
6. Perform the waterflood with field produced water at displacement rate of 2 ft/day for 4 pore volumes.
7. Inject 0.25 pore volume of the preflush solution at 2 ft/day.
8. Inject 0.3 pore volume of the ASP slug at 2 ft/day.
9. Inject 0.7 pore volume of the polymer drive at 2 ft/day.
10. Inject 2 pore volumes of the field produced brine at 2 ft/day.

Table 10 shows the composition of various slugs injected during the coreflood. The pressure drop data was recorded for the whole core as well as that for the five sections during the coreflood. An automated fraction collector was used to collect effluent samples. Surfactant concentration in the effluent samples was measured using high performance liquid chromatography (HPLC) using surfactant plus LC column.

Table 10—Composition of various slugs injected during the coreflood using Berea core.

Characteristic	Pre-flush	ASP Drive	Polymer Drive
Slug Size (PV)	0.25	0.3	0.7
Chemical composition (wt%)	2.5 wt% NaCl	1.75 wt% Na_2CO_3 + 0.9 wt% NaCl	1.9 wt% NaCl
Sacrificial agent conc. (wt%)	1.0	0.5	–
Surfactant conc. (wt%)	–	1.0	–
Polymer (HPAM) conc. (wt%)	–	0.21	0.20
Viscosity (cP)	1	15	15

At the end of the oil injection step, the oil saturation (So) was calculated to be 0.65. During the waterflood stage, the maximum recorded pressure drop was 26 PSI. The waterflood recovery was calculated to be 37% of the original oil in place (OOIP). The residual oil saturation (Sor) was 0.42.

Figure 10 shows the pressure drop recorded during the chemical injection using low permeability (65 mD) Berea core sample. Pressure drop at the end of waterflood was about 26 PSI. During the ASP slug injection, pressure drop steadily increased to about 37 PSI and the peak in pressure drop response was followed by the breakthrough of the oil bank as shown in Figure 11. For the duration of 0.25 PV to 1 PV, residual oil was produced at high oil cut (between 30-45% oil cut). Oil recovery slowed significantly after 1 pore volume of injection. This suggested that the coreflood experiment was run with good mobility control.

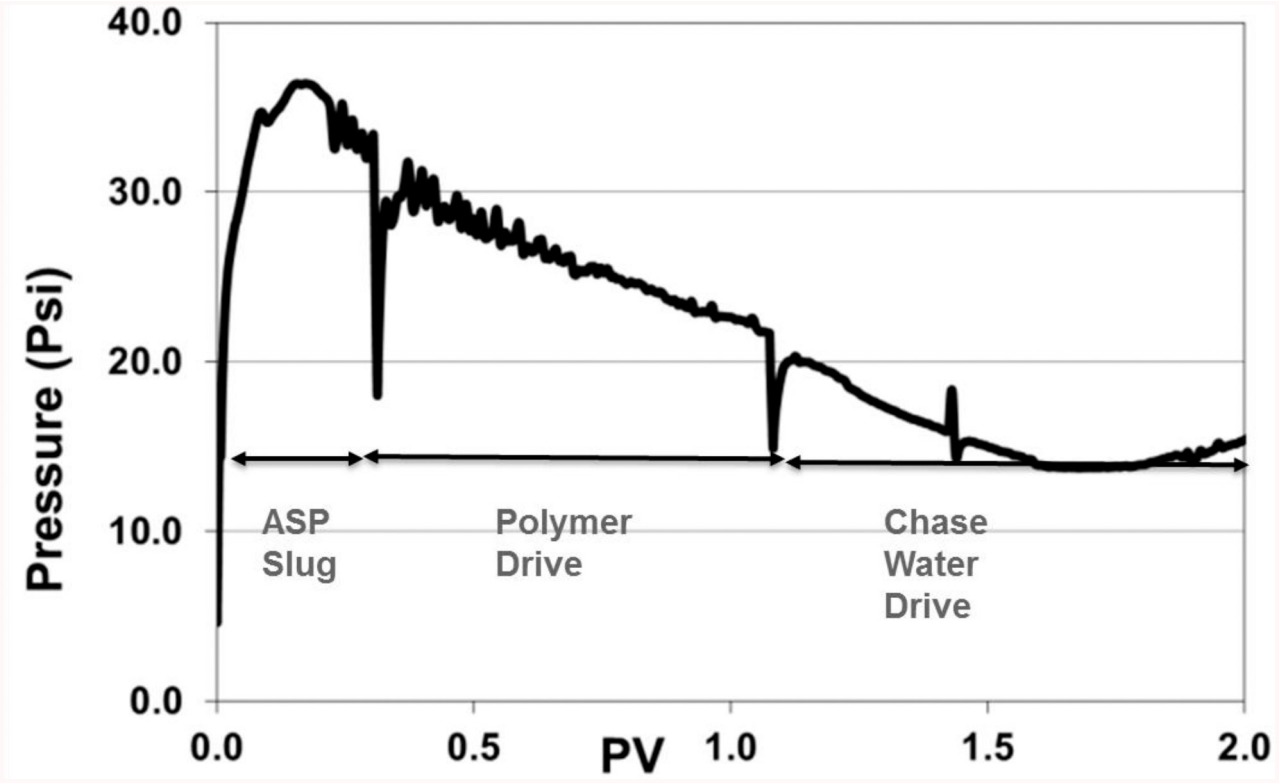

Figure 10—Total pressure drop across the core for the ASP coreflood using 65 mD Berea core. The viscosity of the ASP slug and polymer drive was 15 Cp.

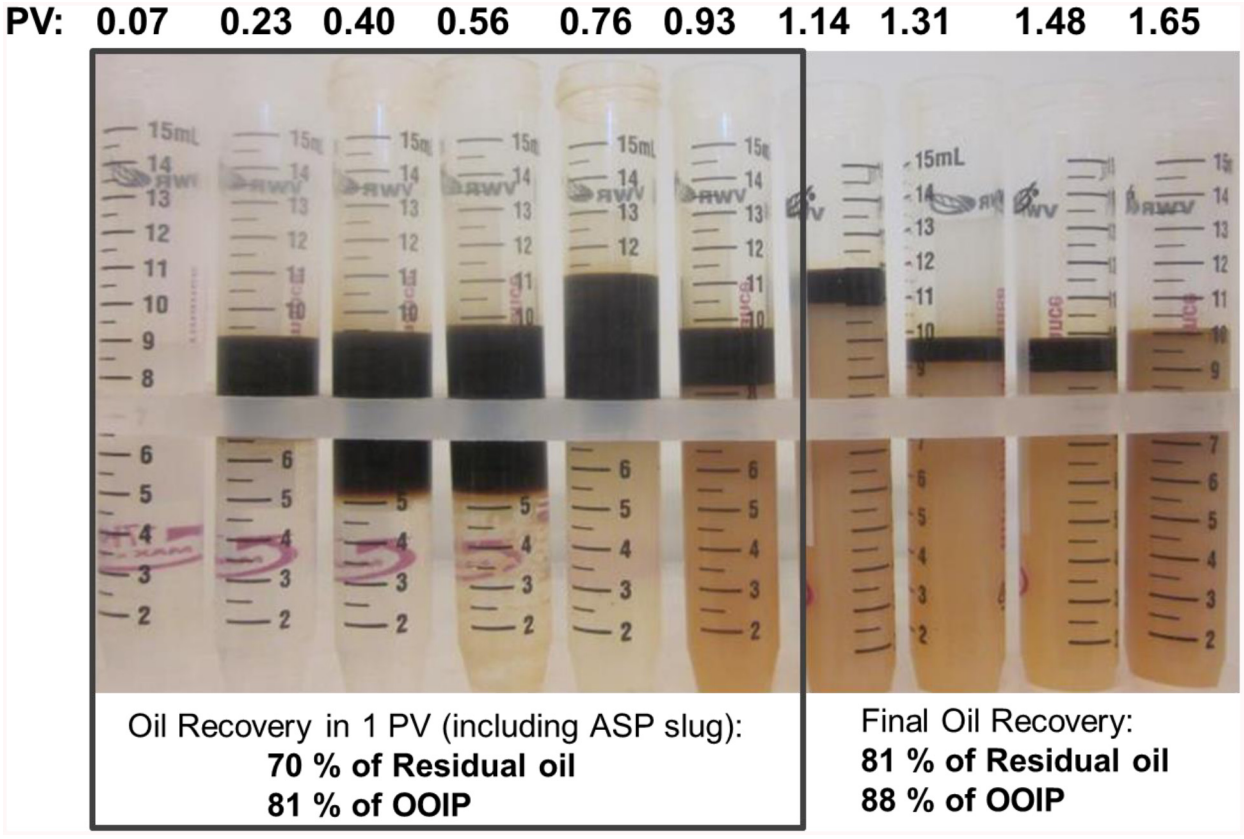

Figure 11—Effluents collected during chemical injection into the Berea core.

Figure 11 shows the effluent samples collected during the chemical injection. The oil and aqueous phase separated rapidly without centrifugation. No emulsion was produced during the coreflood. Figure 12 shows that majority of the oil recovery takes place during first pore volume of the chemical injection. During the first pore volume of chemical injection, about 70% of the residual oil was produced. Final oil recovery (after 2 pore volumes) was 81% of the residual oil. Figure 13 shows the pictures of the Berea core after the completion of the coreflood. No streaks of unswept oil were noticed upon visual inspection.

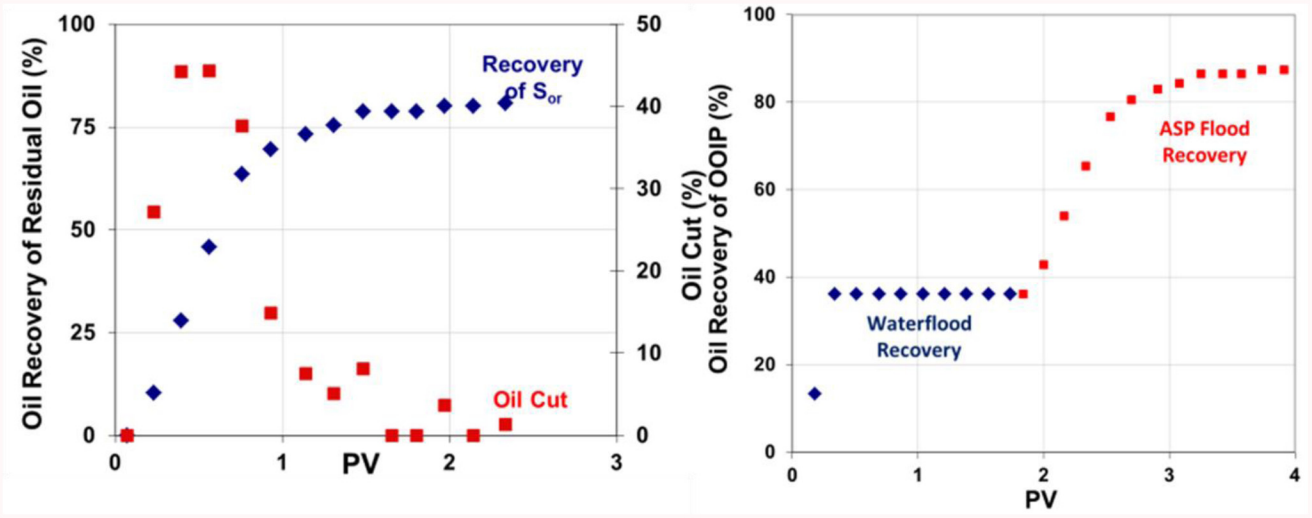

Figure 12—Recovery of residual oil during the coreflood. The plot on the left shows the residual recovery and the oil cut during chemical injection. The plot on the right shows that the waterflood recovery was 37% of original oil in place (OOIP) while the ASP flood recovery was 51% of OOIP.

Figure 13—The Berea core after completion of the coreflood. No streaks of unswept oil were observed upon visual inspection.

Figure 14 shows the surfactant and the sacrificial agent concentrations measured from effluent samples. Breakthrough of both surfactant and sacrificial agent took place at close to 1 PV. First peak in the surfactant concentration is the true breakthrough curve for the surfactant because the second peak can be attributed to the desorbed surfactant during low salinity chase water drive. The maximum surfactant concentration from the breakthrough curve was measured at 1,500 ppm. The maximum sacrificial agent concentration was measured to be about 2,500 ppm. This suggests that enough surfactant and sacrificial

agent were injected. The pore volume of ASP slug and the concentrations of the surfactant and the sacrificial agent in the ASP slug can be optimized in later tests.

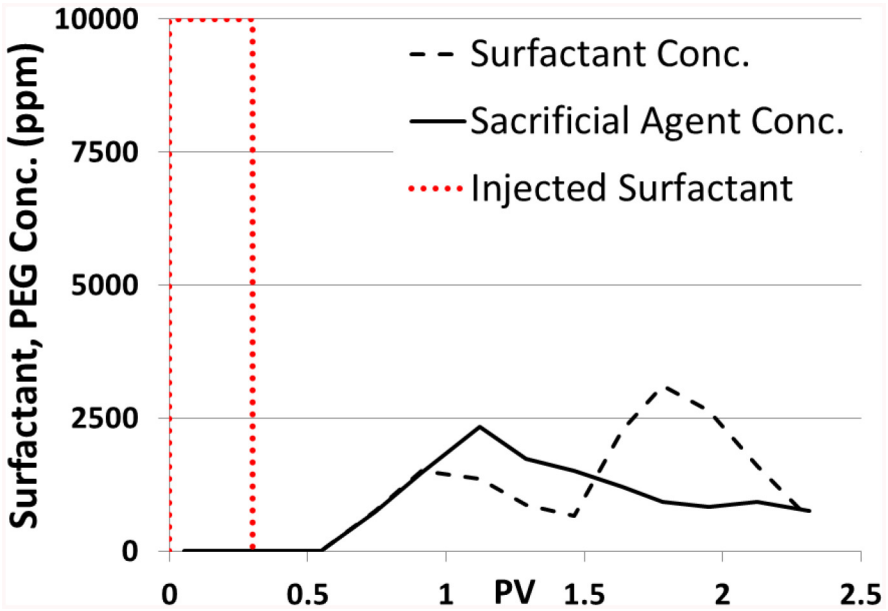

Figure 14—Surfactant and sacrificial agent concentrations measured from the effluent samples using HPLC.

Reservoir rock coreflood: Reservoir core that was used for this project was originally collected between 2006 and 2008 during the drilling of two wells. Historical core analysis data were used to identify appropriate samples for clay analysis. Apart from overall lithologic criteria, samples of similar lithogies having drastically different porosities and permeabilities were selected in order to evaluate the relative percent clay and its effect on reservoir quality. Several factors including historic development, production, depletion, stimulation, and injection have already affected the distribution and the state of clays within the reservoir. As this core was collected after primary and secondary recovery, this core material is likely representative of a clay damaged reservoir.

Limited availability of the representative reservoir core material suggests that a coreflood run with available reservoir coreplugs represents the worst case scenario in terms of permeability and clay content of the reservoir. Because of this, the coreflood performed using reservoir rock coreplugs serves to demonstrate the effectiveness of the formulation in recovering residual oil from low permeability (about 20 mD) composite core in a qualitative sense.

Cleaning of the reservoir coreplugs for restored core analysis: Use of outcrop cores such as Berea doesn't require cleaning of the core sample. However, while using reservoir rock cores it is important to restore the coreplugs to current reservoir conditions prior to chemical injection (Cuiec et al. 1979). Restored state analysis requires that the core be cleaned to the water-wet state that existed before oil accumulated in the formation (Cuiec, 1984; Hirasaki et al. 1990). The core was then saturated with crude oil to a capillary pressure typical of the formation and the system allowed to equilibrate or ″age″ at reservoir temperature.

Typically a refluxing solution of one solvent or an azeotropic mixture of multiple solvents (Toluene, Toluene/Methanol, Chloroform/Methanol etc.) is used to clean cores of residual oil in many universities as well as commercial core analysis labs. In solvent cleaning using a Soxhlet type apparatus, it is assumed that the application of heat, diffusion of solvent and enough cleaning time would ultimately dissolve residual oil from all of the pore space in the core. However, our experience suggests that for low permeability (<30 md) coreplugs such cleaning method is inadequate even after a week long process.

Flow-through cleaning using a variety of solvents is more effective in removing residual oil and returning the coreplugs to water wet state.

Figure 15 shows the collected effluents during the flow-through cleaning using various solvents. The effluents appeared clear of any oil after injecting about 10 pore volumes toluene. However, switching the cleaning solvent to tetrahydrofuran (THF) resulted in a dark black effluent. This confirmed that cleaning of cores using toluene alone was not sufficient. After cleaning with THF, chloroform was used to displace THF from the core. Methanol was then used to displace chloroform from the core (Hirasaki et al. 1990). Finally, excess air (at 135 PSI) was injected through the core to evaporate methanol from the core. The dried core samples were kept under vacuum to remove any residual methanol from the core sample. Afterwards, dry weight, length and diameter of each coreplug were recorded. The coreflood procedure was same as outlined in the previous section of this paper.

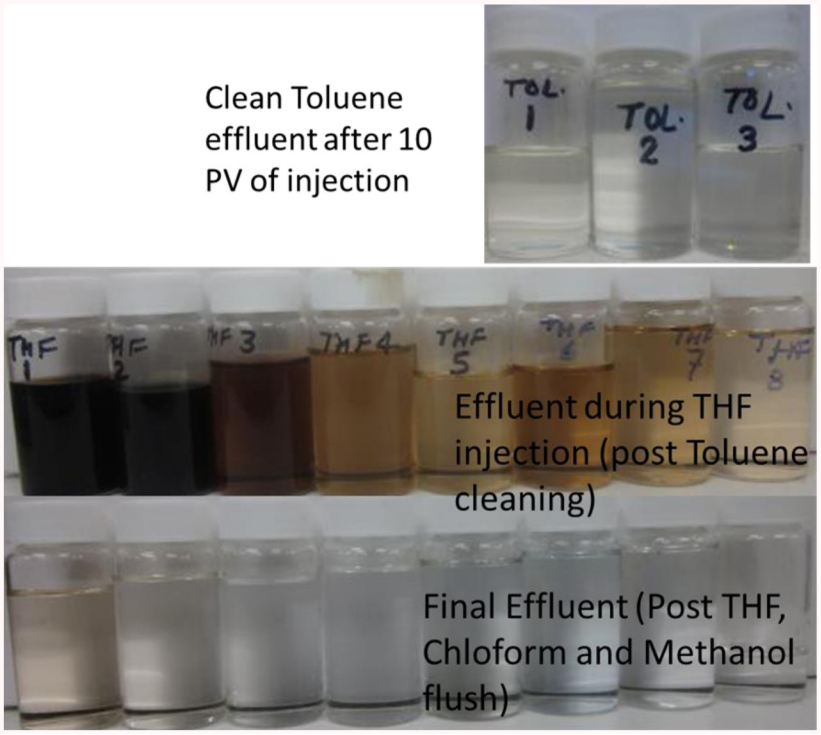

Figure 15—Effluents collected during the flow through cleaning using a variety of solvents.

The permeability of the composite core was calculated to be 20 mD during the brine saturation. Because of low permeability of the core, it was decided to use the lower concentration of lower molecular weight polymer to prevent plugging. The viscosities of the ASP slug and the polymer drive were 10 cP each. Viscosity of the ASP slug and polymer drive may not be sufficient to main good mobility control during the coreflood. However, since they are greater than the viscosity of the crude oil, we did not expect significant fingering through the core during chemical injection. Table 11 lists the composition of the various slugs injected in the core during the coreflood.

Table 11—Composition of various slugs injected during the coreflood using reservoir coreplugs.

Characteristic	Pre-flush	ASP Drive	Polymer Drive
Slug Size (PV)	0.25	0.3	0.7
Chemical composition (wt%)	2.5 wt% NaCl	1.75 wt% Na_2CO_3 + 0.9 wt% NaCl	1.9 wt% NaCl
Sacrificial agent conc. (wt%)	1.0	0.5	–
Surfactant conc. (wt%)	–	1.0	–
Polymer (HPAM) conc. (wt%)	–	0.16	0.16
Viscosity (cP)	1	10	10

At the end of oil injection step, the oil saturation (So) was calculated to be 0.61. During the waterflood stage, the maximum recorded pressure drop was 34 PSI. The waterflood recovery was calculated to be 29% of the original oil in place (OOIP). This low waterflood recovery was consistent with the waterflood recovery observed in the field. At the end of waterflood, the residual oil saturation (Sor) was 0.44.

Figure 16 shows the pressure drop recorded during the chemical injection for the composite core sample. Pressure drop at the end of waterflood was about 34 PSI. During the ASP slug injection, pressure drop steadily increased to about 50 PSI and the peak in pressure response corresponded to the breakthrough of the oil bank as shown in Figure 17. For the duration of 0.25 PV to 1 PV, residual oil was produced at high oil cut (between 22-30% oil cut). Unlike the coreflood using the Berea core, for the composite core the oil recovery did not slow down after 1 pore volume of injection. This suggested that the coreflood experiment was not run with adequate mobility control and some fingering was taking place during displacement. Figure 17 shows that during the first pore volume of chemical injection, about 42% of the residual oil was produced. Final oil recovery (after 2 pore volumes) was 52% of the residual oil. Figure 18 shows the effluent samples collected during the chemical injection. Figure 19 shows before and post chemical flood pictures of the coreplugs used in the coreflood.

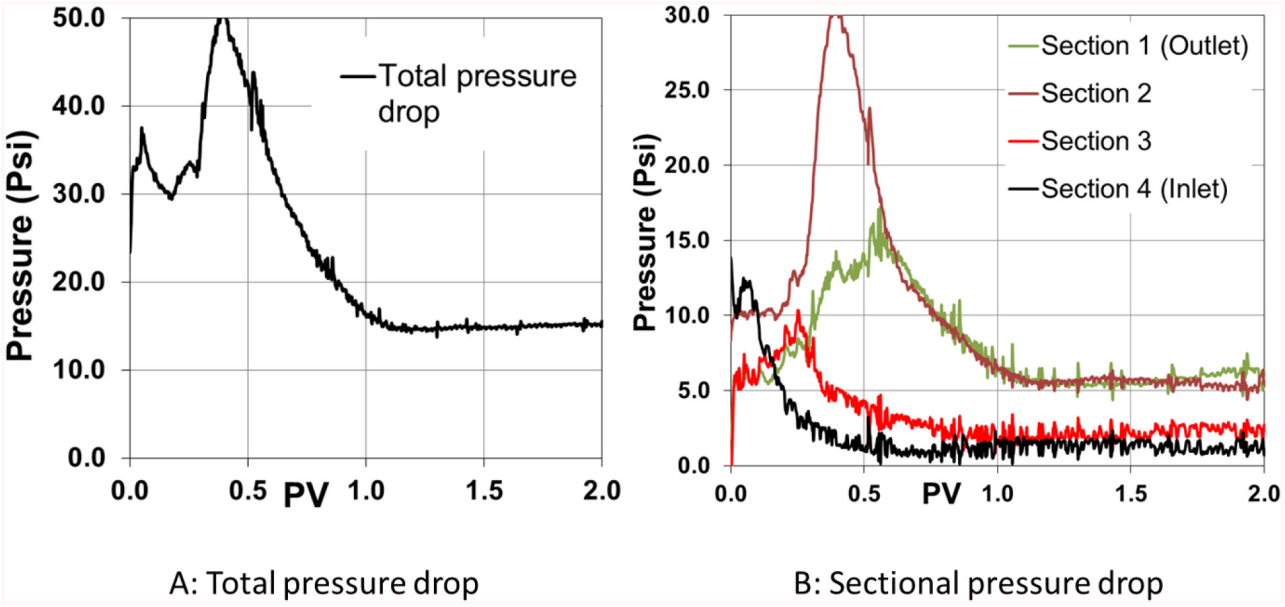

Figure 16—Pressure drop response of the reservoir rock composite core during the chemical injection. Both total and sectional pressure drops are shown.

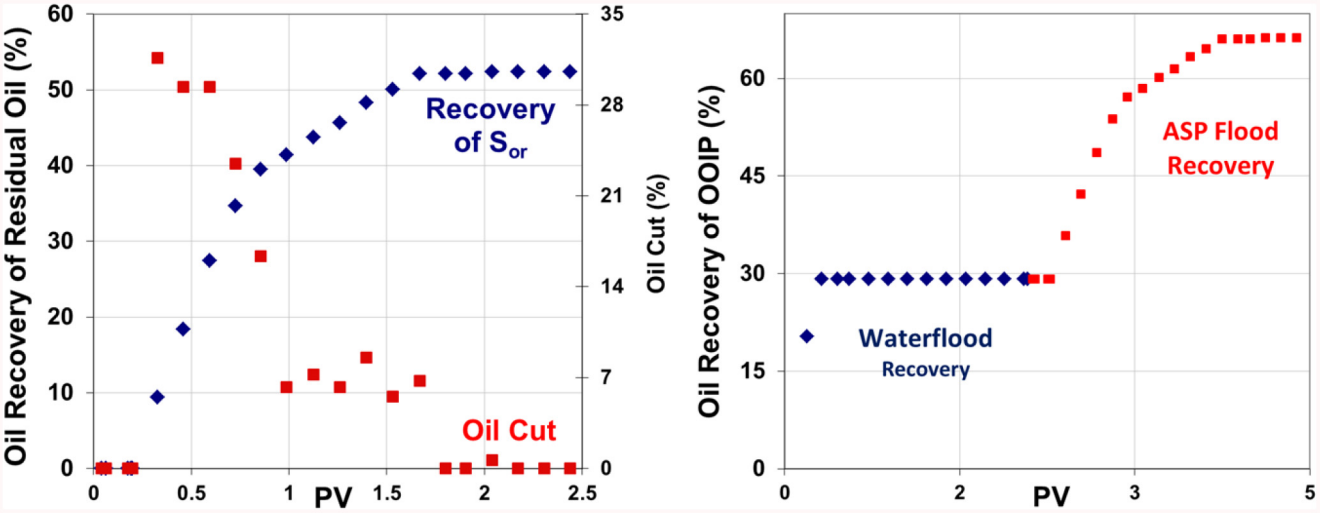

Figure 17—Oil recovery plots showing recovery of residual oil during the coreflood. The plot on the left shows residual recovery and the oil cut during chemical injection. The plot on the right shows the waterflood recovery was 29% of original oil in place (OOIP) while the ASP flood recovered additional 38% of OOIP.

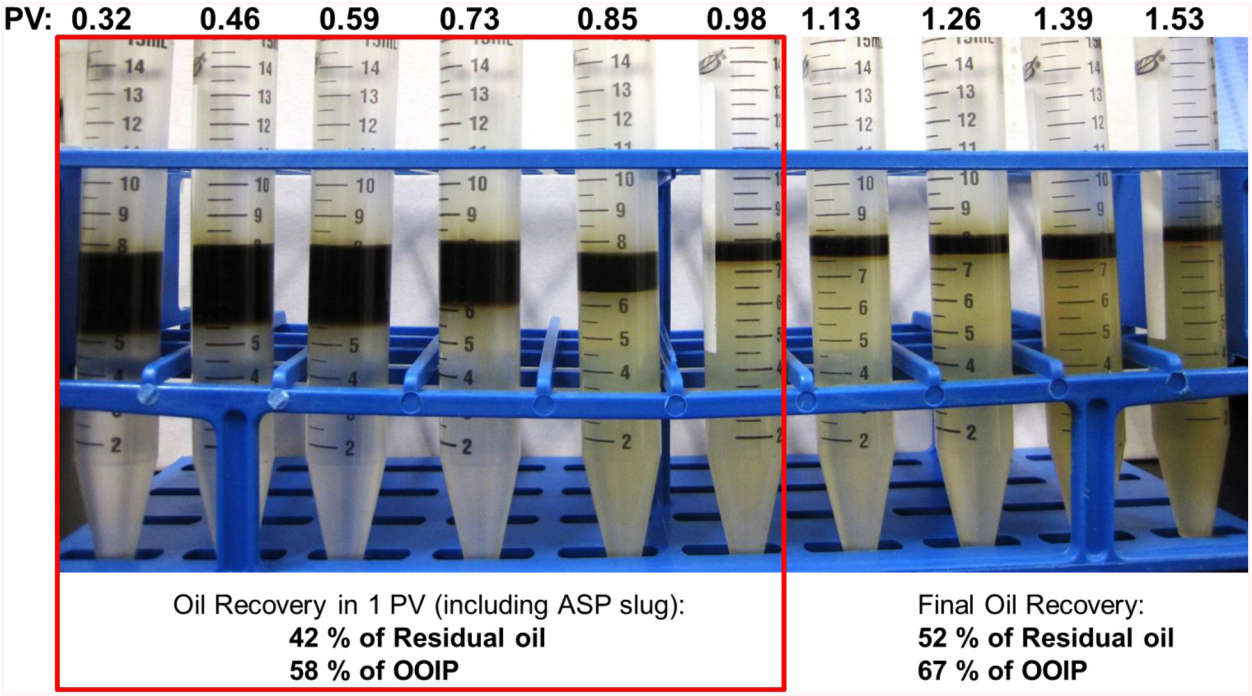

Figure 18—Effluents collected during chemical injection into the reservoir cores.

Figure 19—The reservoir coreplugs before and after completion of the coreflood.

Though, the recovery using the reservoir coreplugs was lower than observed with low permeability Berea core, there may be several reasons for it.

1. Due to low permeability of the reservoir coreplugs (20 mD), some of the pore space may be inaccessible to the ASP slug/Polymer drive solution.
2. Low viscosity of the injected ASP slug and the polymer drive could lead to poor mobility control during the coreflood. This was confirmed by observation that the oil recovery continues after 1 pore volume and small amounts of residual oil was produced through 1.8 pore volumes of chemical injection.

Despite the lower recovery, the reservoir rock coreflood confirmed that the surfactant formulation was able to mobilize significant amount of residual oil and the selected sacrificial agent was highly effective in mitigating surfactant loss due to adsorption on the reservoir rock.

Single well chemical tracer test (SWCTT):

To further test the developed surfactant formulation under field conditions, Chemical tracers, Inc. performed a single well chemical tracer test (SWCTT) at one of the wells in the reservoir. The details of SWCTT can be found in the literature reports (Deans and Carlisle, 1986; Tomich et al. 1973). However, the basic idea of single well tracer test is discussed briefly in this paper for completeness. In a SWCTT, the same well is used as injection and production well at different stages of the test.

1. Excess produced water is injected into the well and is produced back to ensure no free oil is being produced.
2. Chemical tracers are injected into the well and the well is shut in for a period of time.
3. Tracers are produced back and based on the separation of the tracers due to partitioning between the aqueous and the oil phases, the oil saturation is calculated.
4. After the initial oil saturation is measured, ASP chemicals are injected into the well and are chased by excess produced water to push mobilized oil away from the well.
5. Chemical tracer test is repeated to measure the post-ASP oil saturation.

6. Difference between initial and final oil saturation characterizes the effectiveness of the surfactant formulation.

Tables 12 and 13 show the calculated oil saturation before and after the injection of ASP chemicals. The average oil saturation prior to ASP injection was about 0.32. Post ASP injection, the average oil saturation was reduced to 0.10. This shows that in a single well test, ASP chemicals mobilized about 69% of the residual oil making it a successful ASP flood. Further inspection of the SWCT test data suggests that ASP fluid was not able to contact the layer 1 effectively which could be due to inaccessible pore volume for the ASP/Polymer drive. This suggests the need to do a further analysis in finding the suitable molecular weight of polymer which can assist in maximizing the accessible pore space to ASP/polymer drive.

Table 12—Initial oil saturation of the three layers detected as part of pore space.

Layer	Fraction of SWCTT fluid entering layer	Layer Sor
Layer 1	0.16	0.34
Layer 2	0.64	0.37
Layer 3	0.20	0.15
Total	1.00	0.32

Table 13—Oil saturation of the three layers detected as part of pore space after the ASP injection.

Layer	Fraction of SWCTT fluid entering layer	Layer Sor
Layer 1	0.15	0.33
Layer 2	0.65	0.07
Layer 3	0.20	0.03
Total	1.00	0.10

Conclusions

A robust ASP formulation was designed for clay rich and moderarely permeable sandstone reservoir. The key challenge to make an ASP process economical in the field is to reduce the adsorption of the surfactant to acceptable levels. The ASP formulation was proved to be effective using various benchmarking metrics such as:

1. Ultra-low IFT (10^{-3} dynes/cm or lower) over a wide range of salinity (5,000 ppm).
2. Low middle phase microemulsion viscosity (6-11 cP).
3. Low adsorption of surfactant (< 0.5 mg/g rock in static testing) when using an identified sacrificial agent that works in synergy with alkali.
4. Good recovery of residual oil in laboratory corefloods using 0.3 PV of ASP slug at 1.0 wt% total surfactant dose.

Under field conditions, ASP formulation recovered 69% of the residual oil during a single well chemical tracer test. This demonstrates that ASP technology can be applied successfully and economically in targeting clay rich sandstones with low permeability (20-50 md) for enhanced oil recovery.

Acknowledgements

We gratefully acknowledge Wayne Neumiller and Rebecca Podio of Osage Partners, LLC. We also acknowledge our colleagues at TIORCO and at Enhanced Oil Recovery Institute (EORI) at University of Wyoming for many meaningful discussions.

References

Austad, T. 1993. A Review of Retention Mechanisms of Ethoxylated Sulfonates in Reservoir Cores. *Society of Petroleum Engineers*. http://dx.doi.org/10.2118/25174-MS

Bai, B., & Grigg, R. B. 2005. Kinetics and Equilibria of Calcium Lignosulfonate Adsorption and Desorption onto Limestone. *Society of Petroleum Engineers*. http://dx.doi.org/10.2118/93098-MS

Bourrel, M., & Schechter, R. S. 2010. Microemulsions and related systems: formulation, solvency, and physical properties. *Editions OPHRYS*

Cuiec, L. 1984. Rock/Crude-Oil Interactions and Wettability: An Attempt to Understand Their Interrelation. *Society of Petroleum Engineers*. http://dx.doi.org/10.2118/13211-MS

Cuiec, L., Longeron, D., & Pacsirszky, J. 1979. On The Necessity Of Respecting Reservoir Conditions In Laboratory Displacement Studies. *Society of Petroleum Engineers*. http://dx.doi.org/10.2118/7785-MS

Deans, H. A., & Carlisle, C. T. 1986. Single-Well Tracer Test in Complex Pore Systems. *Society of Petroleum Engineers*. http://dx.doi.org/10.2118/14886-MS

Dullien, F. A. L. 1975. Single phase flow through porous media and pore structure. *The Chemical Engineering Journal,* **10**(1), 1–34

Falcone Jr, J. S., Krumrine, P. H., & Schweiker, G. C. 1982. The use of inorganic sacrificial agents in combination with surfactants in enhanced oil recovery. *Journal of the American Oil Chemists Society,* **59**(10), 826A–832A

Gogarty, W. B., Meabon, H. P., & Milton, H. W. 1970. Mobility Control Design for Miscible-Type Waterfloods Using Micellar Solutions. *Society of Petroleum Engineers*. http://dx.doi.org/10.2118/1847-E-PA

Griffith, T. D. 1978. Application of the Ion Exchange Process to Reservoir Preflushes. *Society of Petroleum Engineers*. http://dx.doi.org/10.2118/7587-MS

Healy, R. N., & Reed, R. L. 1974. Physicochemical Aspects of Microemulsion Flooding. *Society of Petroleum Engineers*. http://dx.doi.org/10.2118/4583-PA

Hirasaki, G. J. 1982. Interpretation of the Change in Optimal Salinity with Overall Surfactant Concentration. *Society of Petroleum Engineers*. http://dx.doi.org/10.2118/10063-PA

Hirasaki, G. J., & Pope, G. A. 1974. Analysis of Factors Influencing Mobility and Adsorption in the Flow of Polymer Solution through Porous Media. *Society of Petroleum Engineers*. http://dx.doi.org/10.2118/4026-PA

Hirasaki, G. J., Rohan, J. A., Dubey, S. T., & Niko, H. 1990. Wettability Evaluation During Restored-State Core Analysis. *Society of Petroleum Engineers*. http://dx.doi.org/10.2118/20506-MS

Hirasaki, G. J., van Domselaar, H. R., & Nelson, R. C. 1983. Evaluation of the Salinity Gradient Concept in Surfactant Flooding. *Society of Petroleum Engineers*. http://dx.doi.org/10.2118/8825-PA

Hirasaki, G., Miller, C. A., & Puerto, M. 2011. Recent Advances in Surfactant EOR. *Society of Petroleum Engineers*. http://dx.doi.org/10.2118/115386-PA

Huh, C. 1979. Interfacial tensions and solubilizing ability of a microemulsion phase that coexists with oil and brine. *Journal of Colloid and Interface Science,* **71**(2), 408–426

Jones, N., Chopping, C. & Yin, P. 2013. Core evaluation and clay analysis of the Newcastle Sandstone, Osage Wyoming. *Prepared for Osage Partners, LLC* http://www.uwyo.edu/eori/_files/clayanalysisreport.pdf (accessed 21 January, 2016)

Koopal, L. K., Lee, E. M., & Böhmer, M. R. 1995. Adsorption of cationic and anionic surfactants on charged metal oxide surfaces. *Journal of colloid and interface science,* **170**(1), 85–97

Langmuir, Donald. 1997. *Aqueous environmental geochemistry*. Upper Saddle River, N.J.: Prentice Hall

Liu, S., Zhang, D., Yan, W., Puerto, M., Hirasaki, G. J., & Miller, C. A. 2008. Favorable Attributes of Alkaline-Surfactant-Polymer Flooding. *Society of Petroleum Engineers*. http://dx.doi.org/10.2118/99744-PA

Lopez-Salinas, J. L., Miller, C. A., Koh Yoo, K. H., & Puerto, M. 2009. Viscometer for Opaque, Sealed Microemulsion Samples. *Society of Petroleum Engineers*. http://dx.doi.org/10.2118/121575-MS

Melrose, J. C. & Brandner, C.F. 1974. Role of capillary forces in determining microscopic displacement efficiency for oil recovery by waterflooding. *Journal of Canadian Petroleum Technology,* **13**(04)

Osterloh, W. T., & Jante, M. J. 1992. Surfactant-Polymer Flooding With Anionic PO/EO Surfactant Microemulsions Containing Polyethylene Glycol Additives. *Society of Petroleum Engineers*. http://dx.doi.org/10.2118/24151-MS

Shamsijazeyi, H., Hirasaki, G., & Verduzco, R. 2013. Sacrificial Agent for Reducing Adsorption of Anionic Surfactants. *Society of Petroleum Engineers*. http://dx.doi.org/10.2118/164061-MS

Sheng, J. 2010a. *Modern chemical enhanced oil recovery: theory and practice*. Gulf Professional Publishing

Sheng, J. J. 2010b. Optimum phase type and optimum salinity profile in surfactant flooding. *Journal of Petroleum Science and Engineering,* **75**(1), 143–153

Sheng, J. J. 2013. A Comprehensive Review of Alkaline-Surfactant-Polymer (ASP) Flooding. *Society of Petroleum Engineers*. http://dx.doi.org/10.2118/165358-MS

Somasundaran, P., & Hanna, H. S. 1979. Adsorption of Sulfonates on Reservoir Rocks. *Society of Petroleum Engineers*. http://dx.doi.org/10.2118/7059-PA

Stegemeier, G. L. 1974. Relationship of Trapped Oil Saturation to Petrophysical Properties of Porous Media. *Society of Petroleum Engineers.* http://dx.doi.org/10.2118/4754-M

Stone, W. D. 1972. Stratigraphy and Exploration of the Lower Cretaceous Muddy Formation Northern Powder River Basin, Wyoming and Montana. *The Mountain Geologist,* Vol. **9,** 24p

Taber, J. J. 1969. Dynamic and Static Forces Required To Remove a Discontinuous Oil Phase from Porous Media Containing Both Oil and Water. *Society of Petroleum Engineers*. http://dx.doi.org/10.2118/2098-PA

Tomich, J. F., Dalton, R. L., Deans, H. A., & Shallenberger, L. K. 1973. Single-Well Tracer Method to Measure Residual Oil Saturation. *Society of Petroleum Engineers.* http://dx.doi.org/10.2118/3792-PA

Velde, B. B., & Meunier, A. 2008. *The Origin of Clay Minerals in Soils and Weathered Rocks*: Springer Science & Business Media

Wilson, M. D., & Pittman, E. D. 1977. Authigenic clays in sandstones: recognition and influence on reservoir properties and paleoenvironmental analysis. *Journal of Sedimentary Research,* **47**(1)

Zhang, R., & Somasundaran, P. 2006. Advances in adsorption of surfactants and their mixtures at solid/solution interfaces. *Advances in colloid and interface science,* **123,** 213–229